34th Annual International Conference of the IEEE EMBS
San Diego, California USA, 28 August - 1 September, 2012

Subpeak Regional Analysis of Intracranial Pressure Waveform Morphology based on Cerebrospinal Fluid Hydrodynamics in the Cerebral Aqueduct and Prepontine Cistern

Robert B. Hamilton, Kevin Baldwin, Paul Vespa, Marvin Bergsneider, Xiao Hu

Abstract— **The objective of this study is to investigate the relationship between intracranial pressure (ICP) pulse waveform morphology and selected hydrodynamic metrics of cerebrospinal fluid (CSF) movement using a novel method for ICP pulse pressure regional analysis based on the Morphological Clustering and Analysis of Continuous Intracranial Pulse (MOCAIP) algorithm.**

Methods: Seven patients received both overnight ICP monitoring along with a phase contrast MRI (PC-MRI) of the cerebral aqueduct and prepontine cistern to measure peak velocity, peak to peak mean flow, and stroke volume. Waveform morphological analysis of the ICP signal was performed by the MOCAIP algorithm. Following extraction of morphological metrics from the ICP signal, each ICP metric (128 metrics) was compared to each CSF metric via Spearman's rank correlation. The ICP results were further analyzed using a binary scheme which assigned the individual metrics a regional contribution based on the characteristic triphasic ICP pulse waveform.

Results: All three aqueductal CSF metrics were shown to be significantly correlated with region 2 of the triphasic ICP pulse pressure waveform. Furthermore, the prepontine cistern showed two significant correlations between the CSF metrics and region 3 of the ICP waveform.

Conclusion: In this study we showed that non-invasive measures of CSF movement in two different anatomical locations are significantly related to different sub-peak regions of the ICP pulse pressure waveform.

I. Introduction

The objective of this study is to investigate the relationship between intracranial pressure (ICP) pulse waveform morphology and selected hydrodynamic metrics of cerebrospinal fluid (CSF) movement using a novel method for ICP pulse pressure sub-peak regional analysis. Our interest in ICP waveform analysis stems from a long-term goal to advance ICP monitoring by delivering more clinically useful metrics in addition to mean ICP (mICP), which remains the only parameter reported to clinicians by current ICP monitors. To reach this goal, our group and other colleagues have done a series of work in advancing the techniques of ICP signal analysis [1, 2]. One specific example is the Morphological Clustering and Analysis of Continuous Intracranial Pulse (MOCAIP) algorithm [1] through which one can first robustly identify the locations of the three sub-peaks and valleys of an ICP pulse and then systematically extract 128 metrics that characterize the amplitude, curvature, slope, and time intervals among these landmarks. Several studies have been performed which show the benefits ICP morphological analysis and the MOCAIP algorithm [3, 4]. However, this study extends MOCAIP analysis to infer relationships for the different sub-peak regions in the triphasic ICP waveform; which we believe will lead to a greater understanding physiologically of the ICP pulse pressure waveform and thus a more advanced ICP monitoring system.

To test the ability of the MOCAIP metrics to characterize different sub-peak regions of ICP we have selected three non-invasive hydrodynamic variables measured by phase contrast MRI (PC-MRI) in the cerebral aqueduct (aqueduct) and the prepontine cistern (cistern). The aqueduct and cistern represent locations in two complementary compartments of the cranial vault, the ventricular system and the subarachnoid space, respectively. Our objective is to determine if the CSF hydrodynamics metrics from the aqueduct and cistern are significantly related to any of the sub-peak regions of the ICP waveform.

II. Methods

A. Patient Characteristics & Data Acquisition

Seven patients (71.1 ± 9.8 years) were under evaluation for normal pressure hydrocephalus (NPH) at the UCLA Adult Hydrocephalus Center and received both a PC-MRI CSF flow protocol and overnight ICP monitoring. The local IRB approved all data acquisition and all subjects signed informed consent to participate.

Intracranial Pressure Monitoring

An intraparenchymal ICP microsensor (Codman and Schurtleff, Raynaud, MA) was inserted in the right frontal lobe and continuously monitoring ICP one night before the placement of the lumbar drain (LD). Continuous waveform data including ECG and ICP was captured using the BedMaster™ (Excel Medical Electronics, Inc. Jupiter, FL) system with a sampling rate of 240 Hz.

Phase-Contrast MRI Protocol

All seven patients underwent the PC-MRI CSF flow protocol. The imaging either preceded admission for the extended lumbar drain (ELD) trial or followed the ELD by no less than three weeks; which allowed for equilibration of

*Work partially supported by NS059797, NS054881, and Ns066008

Robert .B Hamilton (RHamilton@medne.ucla.edu), Kevin Baldwin (KBaldwin@mednet.ucla.edu), Xaio Hu (XHu@mednet.ucla.edu), Marvin Bergsneider (MBergsneider@mednet.ucla.edu), are with the Neural Systems and Dynamics Laboratory, Department of Neurosurgery, University of California, Los Angeles.

Paul Vespa (PVespa@mednet.ucla.edu) is with the Neurocritical Care Program, Department of Neurosurgery, University of California, Los Angeles.

the baseline hydrodynamics. All MRI scans were performed using a 3 Tesla Siemens Trio T-class MRI (Sienmens Medical Systems, Erlanger, Germany). Phase-contrast imaging took place in the cerebral aqueduct and the prepontine cistern (Fig. 1). For each location the following anatomical sequences were acquired: 3D axial T1-weighted MPRage (0.84375mm/0.899mm, resolution/slice thickness) and a sagittal T2-weighted Turbo spin echo (TSE) sequence (0.34375mm/8mm).

A standard phase contrast sequence (0.625 mm/3 mm) was used for flow quantification in both locations using an oblique plane defined perpendicular to the presumed direction of CSF flow. A flow scout was used to aid the manual determination of the velocity encoding parameter (V_{enc}) to reduce aliasing. Due to the location of the Basilar Artery in the prepontine cistern, a Time-of-Flight (TOF) sequence was used to aid in the segmentation of arterial blood flow from the phase contrast sequence (0.78 mm/0.8 mm). Finally, all phase contrast sequences had a 30 frame temporal resolution retroactively gating with either ECG or pulse oximetry signal.

A. Data Analysis

CSF Hydrodynamic Analysis

A semi-automated segmentation algorithm was implemented in MATLAB 7.5 R2007b (The MathWorks, Inc., Natick, MA, USA) to define the region of interest (ROI) for both anatomical locations [5]. Next, three CSF hydrodynamic metrics were calculated based on the extracted ROI, including the peak velocity, the peak to mean flow (P2P Mean Flow) which represented the absolute mean difference between the average flow rates in the caudal and cranial directions, and the average stroke volume defined as the average of the volume of CSF moving cranial-caudal during systole and that moving caudal-cranial during diastole.

ICP Analysis

The ICP analysis was done using the MOCAIP algorithm developed by our group using MATLAB 7.5 R2007b [1]. MOCAIP is an end-to-end framework devoted to real time time-domain analysis of intracranial waveform morphology. MOCAIP utilizes a five step process to convert the raw ICP and ECG inputs into a series of clean ICP pulses, known as dominant pulses. First, the raw ICP data is segmented using the RR interval of the ECG signal. Following the segmentation, the individual pulses are grouped based on a pre-defined time interval (one minute in this study) and then clustered using a hierarchical clustering method. A dominant pulse is defined for each segment (one minute of raw signal) as the mean of the largest cluster. However, the dominant pulse produced could be an invalid ICP pulse because the entire segment could be noise; therefore, the segment's dominant pulse is checked against a reference ICP pulse library to determine the legitimacy of the pulse. Once the dominant pulse has been verified, six landmarks are determined, the three characteristic peaks and their corresponding valleys. Finally, the algorithm extracts 128 MOCAIP metrics based on the six landmarks for each dominant pulse, an example of the dominant pulse along with sub-peak regions are shown in Fig. 2.

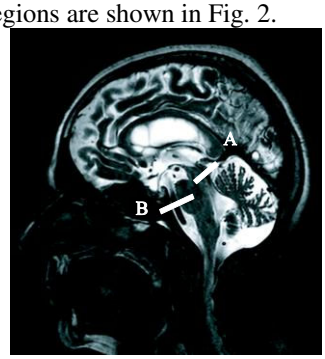

Fig. 1: *Location of the oblique slices for the PC-MRI study,* ***A)*** *cerebral aqueduct and* ***B)*** *the prepontine cistern.*

Description of Region Weight

Although physiologic relationships can be speculated from the individual metrics derived from the MOCAIP algorithm, a more general analysis is possible. The MOCAIP metrics can be divided into sub-peak regions (region 1, 2, and 3), based on a binary scheme that characterizes each MOCAIP metric's dependency on three different sub-peak regions (Fig.2). For example, amplitude metric '**dP1**' (amplitude of the first peak) would be associated with a sub-peak region binary code (1 0 0) representing (region 1 region 2 region 3), where ratio metric **'RCurvp2Curvp3'** (ratio between curvature of peak 2 and curvature of peak 3) would be assigned a code (0 1 1). The sub-regions are not uniformly distributed, with region 1, 2, and 3 having an approximate distribution of 35.6%, 33.2%, and 31.2%, respectively.

Correlation of ICP Metrics and MRI metrics

Following calculation of the metrics sets (PC-MRI and ICP) Spearman's rank correlation coefficient (ρ) was used to quantity the dependencies of the ICP metrics and the hydrodynamic metrics derived from PC-MRI. In other words, each ICP metric (128 metrics, each with a three digit binary region code) was compared to the six aforementioned PC-MRI metrics (three for each of the two locations) and the correlation coefficient was calculated.

Once the correlation coefficients were calculated for each pair of measurements, a threshold value (alpha) had to be determined to study the region contribution of those highly correlated metrics. Namely, each combination will have some correlation value; however, many of these will have correlation coefficients near zero and thus should not be included in the analysis. To investigate the region contribution of the CSF hydrodynamics metrics, an alpha value was determined ad hoc. At this value of alpha, a normalized region contribution (NRC) was calculated; for example, if three metrics had correlation values greater than alpha (dP1, Lv1p3, and mICP: (1 0 0), (1 0 1), (1 1 1), respectively) the NRC would be (47.2% 16.9% 35.9%). Obviously, the NRC is a function of the alpha value, the lower the alpha value the more metrics included in the NRC calculation. To account for this, the NRC was calculated for each alpha value from 0.1 to 1.0 (steps of 0.01) resulting in a

percent region weight trend for each of the three regions. This plot aided in the selection of the final alpha value (Fig. 3).

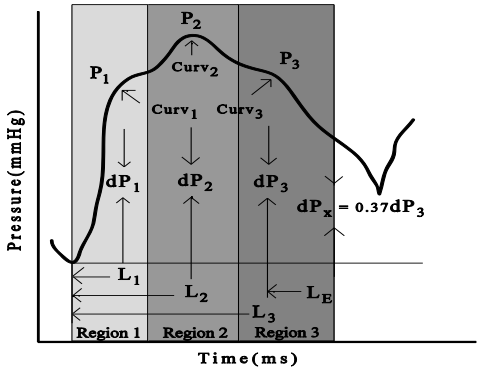

Fig. 2: *MOCAIP example of a dominant pulse with metric identifies including amplitude, latency, and curvature. The regions are also shown in boxes*

To summarize, each of the six CSF metrics were compared to the 128 ICP MOCAIP metrics and a correlation value was calculated. An alpha value was then determined based on the overall distribution of region weights (see Fig. 3). This selection resulted in a small number of ICP metrics (N_{ICP}) that were greater than the alpha value. From the N_{ICP} metrics a NRC was calculated.

For significance testing of the association between a CSF hydrodynamic metric and an ICP pulse sub-peak region, a surrogate data set was used with a significance level of 5%. For any given experiment a number of metrics will be greater than alpha (N_{ICP}). For the surrogate testing, N_{ICP} metrics were randomly selected from the 128 metrics and the NRC was calculated. For example, if the following three metrics were selected (N_{ICP} = dP1, Lv1p3, and mICP) during the initial analysis (Spearman's value greater than alpha), then three metrics would be selected at random from the 128 overall metrics and the NRC would be calculated (N_{random}). To provide an adequate distribution, 10,000 random selections were made. If the NRC calculated from the data (N_{ICP}) was greater than 95% of the randomly generated surrogate data, it was considered significant.

III. Results

For the seven patients a total of 2,785 dominant ICP pulses were analyzed. The results had a mean and standard deviation of 397.9 ± 95.8 dominant pulses per patient, with a range from 209 to 503 pulses. The PC-MRI results for the CSF hydrodynamics are shown in Table 1.

Table 1: *PC-MRI results for the four CSF hydrodynamic parameters for each anatomical location (mean* ± standard deviation)

	Aqueduct	Cistern
Peak Velocity (cm/s)	13.24 ± 4.37	5.54 ± 2.48
P2P Mean Flow (mL/min)	2.99 ± 1.01	1.20 ± 0.77
Stroke Volume (mL)	0.16 ± 0.04	0.24 ±0.09

Regional Analysis

For the aqueduct, all three of the CSF metrics reached significance in regional testing. Peak velocity, P2P Mean Flow, and the aqueductal stroke volume were all significantly correlated with region 2 (Table 2). Although the individual ICP metrics (N_{ICP}) are not reported for each significant correlation it is worth noting that mICP was not included; however, the amplitude of the ICP pulse pressure (waveAmp) was selected for the aqueductal stroke volume and peak velocity.

The prepontine cistern had two CSF metrics reach significance (peak velocity and P2P Mean Flow). Although the stroke volume did not reach significance it maintained the same tendency toward region 3 as the other metrics. Again, mICP was not included as one of the significant ICP metrics.

Threshold Selection

The threshold selection process was based on the trend of the NRC for each alpha value ranging from 0.1 to 1.0 (Fig. 3). Each alpha value in the trend plot has a number of metrics associated with it (N_{ICP}); this is not represented in the figure but is critical for significance testing. The individual alpha values have no physical representation but are reported for completeness in Table 2. An example of the aqueductal P2P Mean Flow regional contribution (percent region) as a function of alpha value is shown in Fig. 3.

Table 2: *Metrics for ICP, PC-MRI, and TCD that were used in the region analysis. Each noninvasive metric (PC-MRI and TCD) was compared against all 128 MOCAIP metrics. *P-value < 0.05 and ** P-value < 0.001*

	Cerebral Aqueduct		Prepontine Cistern	
	Alpha	Region	Alpha	Region
Peak Velocity	0.79	2**	0.64	3*
P2P Mean Flow	0.83	2**	0.46	3*
Stroke Volume	0.58	2*	0.50	3

IV. Discussion

The impact of this study is multifaceted, contributing both technically and physiologically to the study of intracranial pressure and cerebral dynamics. Technically, this study introduces a novel framework for generalizing the ICP morphological metrics produced by the MOCAIP algorithm into regional information based on the characteristic peaks. In this study we proposed the use of CSF hydrodynamics measurements via PC-MRI; however, this framework could easily be expanded to include different measures of brain pulsatility. Physiologically, this work supports the idea global mean value of ICP and the characteristics of the three individual regions of an ICP pulse may reflect different aspects of the CSF dynamics and can provide complementary information. Such a finding therefore challenges the current paradigm of monitoring only mICP while ignoring the shape of an ICP pulse and could have a far researching impact on the study of ICP waveform morphology in a variety of conditions.

Traditional Analysis of ICP

The MOCAIP algorithm provides a framework for the advanced analysis of ICP waveform morphology which has been shown to be advantageous over the traditional mICP in

several conditions. For example, Eide *et al.* has recently shown the prognostic value of ICP pulse amplitude for shunt outcome prediction in NPH patients [6]. The work described in this study extends the morphological metrics by strategically segmenting the 128 metrics into regional contributions seen in Fig. 2. This simple binary framework was developed to help elucidate some of physiological meanings of the MOCAIP metrics. The motivation behind this work is based on the classical studies of ICP waveform morphology that focused on the characteristic peaks.

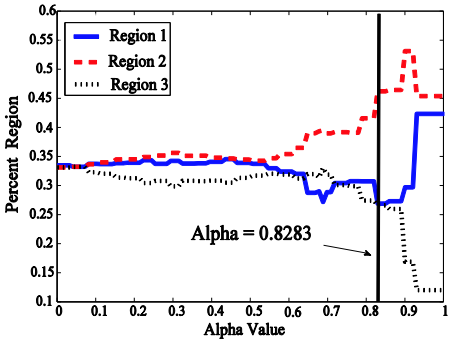

Fig. 3: *Percent region contribution as a function of the alpha value. The plot represents P2P Mean Flow in the cerebral aqueduct. The respective alpha value (where the significance testing was performed) is shown with a vertical line.*

Physiological Impact

Furthermore, the findings in this study provide additional evidence that the sub-peaks of the ICP waveform have physiologic meaning. There are several studies stating theories for each of the characteristic peaks; for P1 (percussion wave), a majority of the literature cites the pulsation of the large intracranial conductive vessels as the main driving force [7]. The second sub-peak (P2) has been linked to capillary expansion. Finally, P3 is thought to be venous in origin [7]. These results have been echoed in recent studies and are accepted as ICP dogma regarding the characteristic peaks.

A key finding of this work is that a significant association exists between CSF hydrodynamic measures from two distinct anatomical locations (aqueduct and cistern) and the sub-peak regions of the ICP pulse. The aqueductal CSF metrics were correlated with region 2 of the ICP waveform. One possible interpretation for these results is that the driving pressure required to displace an increased CSF volume through the aqueduct is related to the second peak of the ICP pulse. Another related theory proposed by Greitz *et al.* suggests that the aqueductal egress is predominantly caused by the brain expansion (capillaries) [8]. Therefore, the second peak of an ICP pulse may correlate with the arterial pulse wave reaching the level of the choroid plexus and/or capillary expansion in terms of the timing.

The results for the prepontine cistern are just as compelling with two CSF metrics significantly correlated with region 3. Traditionally, region 3 has been associated with the venous system. However, we know from previous studies by Greitz and Wagshul *et al.* that the cisternal CSF pulse precedes the aqueductal pulse. Based on these studies the cisternal correlation with region 3 seems paradoxical as one might expect a correlation with region 1. We believe that these results can be explained by the pulsatile nature of CSF. Again, physiologically the ICP pulse pressure waveform is created by the intracranial volume increase from the arterial blood entering the cranial vault. For adequate perfusion of the brain to occur, there must be a CSF egress into the spinal canal and a subsequent return following venous drainage. We believe that the correlation with P3 region is due to the return of CSF back into the cranial vault.

V. Conclusion

In this study we introduced a novel framework for investigating regional attributes of the ICP waveform based on the MOCAIP metrics. Specifically, we measured three CSF hydrodynamic metrics at two distinct locations within the cranial vault (aqueduct and prepontine cistern) and correlated them with ICP morphological metrics derived by the MOCAIP algorithm. We found significant correlations between CSF flow dynamics at both the aqueduct and the cistern correlating with region 2 and region 3 of the ICP pulse waveform, respectively. Although the individual metrics of ICP were not specifically investigated, this work lays the foundation for further study regarding ICP waveform morphology. Although there is a large number of existing studies on both ICP and CSF hydrodynamics, this work for the first time is able to quantitatively assign a relationship of a non-invasive metric to a specific region of the invasive ICP measure. Understanding physiological origins of the waveform shape could lead to greater insights and adoption of ICP waveform morphology.

References

[1] X. Hu, P. Xu, F. Scalzo, P. Vespa, and M. Bergsneider, "Morphological clustering and analysis of continuous intracranial pressure," *IEEE Trans Biomed Eng,* vol. 56, pp. 696-705, Mar 2009.

[2] M. Czosnyka, P. Smielewski, P. Kirkpatrick, R. J. Laing, D. Menon, and J. D. Pickard, "Continuous assessment of the cerebral vasomotor reactivity in head injury," *Neurosurgery,* vol. 41, pp. 11-7; discussion 17-9, Jul 1997.

[3] X. Hu, P. Xu, D. J. Lee, V. Paul, and M. Bergsneider, "Morphological changes of intracranial pressure pulses are correlated with acute dilatation of ventricles," *Acta Neurochir Suppl,* vol. 102, pp. 131-6, 2008.

[4] S. Asgari, M. Bergsneider, R. Hamilton, P. Vespa, and X. Hu, "Consistent Changes in Intracranial Pressure Waveform Morphology Induced by Acute Hypercapnic Cerebral Vasodilatation," *Neurocrit Care,* Oct 29 2010.

[5] R. Hamilton, J. Dye, A. Frew, K. Baldwin, X. Hu, and M. Bergsneider, "Quantification of Pulsatile, Cerebrospinal Fluid Flow within in the Prepontine Cistern," *Acta Neurochir Suppl,* vol. 114, 2011.

[6] P. K. Eide and W. Sorteberg, "Diagnostic intracranial pressure monitoring and surgical management in idiopathic normal pressure hydrocephalus: a 6-year review of 214 patients," *Neurosurgery,* vol. 66, pp. 80-91, Jan 2009.

[7] O. Hirai, H. Handa, M. Ishikawa, and S. H. Kim, "Epidural pulse waveform as an indicator of intracranial pressure dynamics," *Surg Neurol,* vol. 21, pp. 67-74, Jan 1984.

[8] D. Greitz, R. Wirestam, A. Franck, B. Nordell, C. Thomsen, and F. Stahlberg, "Pulsatile brain movement and associated hydrodynamics studied by magnetic resonance phase imaging. The Monro-Kellie doctrine revisited," *Neuroradiology,* vol. 34, pp. 370-80, 1992.